THE *DRAFT* ROTSE PAPER TITLE

Abstract

Abstract: The study of variable stars is a field that is constantly being updated and added to as surveys both new and old release information to the public. In order to consolidate the information that was being catalogued in multiple different locations, the Variable Star Index (VSX) was created. This formed a global, up to date repository that could be added to and modified at a moment's notice through moderator approval. As the data releases expanded upon the amount of available information, so did the amount of interested contributors, which ranged from amateur astronomers to professional physicists. Southern Methodist University contributed its own resources to the effort, and here we present the results and future prospects of an optical-band variable star search using the ROTSE-I and ROTSE-III telescopes, which includes updates and new data submissions to the International Variable Star Index in conjunction with data from other surveys. These stars all feature short timescale optical-light variations, and are described by the magnitude range, period, epoch and variability type that we submit in accordance with supporting data.

Methods: The Robotic Optical Transient Search Experiment (ROTSE) telescopes were originally designed to search for optical light signals from Gamma Ray Bursts (GRBs), but their purpose was later expanded to search for other light sources, to include variable stars. The data sets analyzed in this study run from 1999 to 2000 for ROTSE-I and 2003 onwards for ROTSE-III. Data captured by telescope CCDs was processed by the ROTSE data acquisition pipeline regardless of which telescope was in use. This included data manipulation such as flat field corrections, dark frame subtractions, source extraction and then on to preliminary image calibration. The ROTSE pipeline used image subtraction to amplify subtle changes in an image and separate a source from background noise. The source extraction process then mapped coordinates to light sources, which were tracked across multiple images and multiple nights. Multiple pairs of images could then compiled into match structures which contain data about sources based on the tracked object position. Creating these match structures allowed us to follow the intensity variations that a given celestial object may display while referencing their astrometric, photometric and auxiliary data. This data can then be extracted and passed through statistical cuts based on user input. This process creates lightcurves from single observation periods that can be inspected visually for signs of variation. Any lightcurve that displays a tendency or possibility to vary in visual output is passed through a phasing process in order to determine the variable star's period and amplitude.This was accomplished through a cubic spline fit algorithm developed by University of Michigan astronomer Carl Akerlof and his research team specifically for variable star analysis [**Akerlof**]. Once a properly phased lightcurve was produced, the star's variability type could be narrowed down using period, amplitude and lightcurve shape. Supporting datasets from other telescopic surveys were then phased in with the original lightcurve to provide additional information on variation trends. The fitted data, upon being combined with other sources, was submitted to VSX for moderator review with the eventual goal of a new variable star discovery.

Results: Approximately 350 different variables were found. Of the number encountered, 210 were previously discovered, 80 remain candidates. Previously discovered variables were also updated with type and phase plot information from our survey. At the end of the effort 82 ROTSE-I variables were accepted into the database, along with 20 ROTSE-III variables. Several different variable types were discovered, both intrinsic and extrinsic: 4 RRC variables, 2 RRABs, 7 DSCTs, 2 HADS, 57 EWs, 8 ELLs,

8 EBs, 10 EAs, 2 Es, and 2 CWBs. The vast majority of discoveries were stars in binary systems, with only 17 pulsators amongst the 82 discoveries.

1. Introduction

There are currently more than 465,000 variable stars cataloged in VSX. Each of these entries has a variability type assigned to it, which designates what type of star it is, and denotes the mechanics behind the star's variation in brightness over time. Studying variable stars helps the scientific community learn about physical processes in foreign environments: binary stars such as NL Cataclysmic type variables form accretion disks and can help us study the traits of larger scale accretion physics, such as in neutron stars, white dwarves and even black holes. EW variables were among the first type of variables to have a color-period relation established, opening a new way to characterize different types of stars [**O.J Eggen source**]. The majority of recent discoveries came in the form of EW variables, which have their own characteristics that can contribute to exploration of other astrophysical processes. Close Contact Binaries can be used to study other close contact phenomena such as Type I-a supernova. WUma variables exchange material through a lagrange point until thermal equilibrium is reached. In the same way, Type I-a supernova feature the exchange of matter until a stellar explosion occurs. Thus, the EW star can serve as a small scale model of a supernova process. Additional scientific utility outside of basic discovery and cataloging also holds true for pulsating stars such as Cepheid variables, as they are similar in function to SN Cataclysmic types which provide accurate distance measurements and are used within the Cosmic Distance Ladder. Mira type variables describe a class of pulsating red giants that are in the late stages of stellar evolution and could come to emulate the end of our own Sun's life cycle.

Reporting on the characteristics and location of all these different variable types allows for follow-up studies on these stars through both the amateur and professional astronomy communities. SMU was able to analyze portions of the night sky by a now decommissioned ROTSE-I, and its successor ROTSE-III. The primary mission of the ROTSE telescopes is a search for untriggered gamma-ray bursts. Although not the original intention, an all-sky survey was conducted with both ROTSE-I and ROTSE-III with an objective of searching for periodic variable stars and other astrophysical transients. ROTSE-I data was first analyzed in a demonstration project yielding the discovery of 1781 new variable stars. At the time, it was estimated the entire project could produce more than 32,000 new periodic variables [5]. This potential launched the Variable Star Project (VSP) which has been expanded to include ROTSE-III with the new discovery of several, non-cataclysmic type variable stars. Since ROTSE-I was deactivated, its observations were mined, and metadata was extracted through the use of various analysis techniques**.** The identification of potential variable stars was then done by manual inspection of light curves generated. After many iterations, the process of identifying and submitting variable candidates to the International Variable Star Index (VSX) was improved to a level where the method could be taught and passed down to undergraduates in the field. A similar process to the one used for the analysis of the ROTSE-I data was tested on ROTSE-III data with a previously undiscovered non-CV type variable. ROTSE-III J180829.49-203047.8, was the prototype for the expansion of the VSP into ROTSE-III's data collection. Advancements in the process of analyzing scheduled fields have been made with the hope of achieving the same automation as the discoveries made with ROTSE-1. The challenge experienced with advancing the VSP to ROTSE-III primarily deals with finding an optimal way to create a ROTSE match structure from raw images taken during patrolling nights. The aim of the VSP itself is the systematic identification, analysis, and submission of new variables from existing survey data as well as updating known catalogued variables with a previously unknown type, as some submissions in VSX are incomplete or outdated and have elements that could be improved upon. The focus of this paper will be on the process and results of the VSP.

2. Observations and Data Reduction

2.1 ROTSE-I operation

Located in Los Alamos, New Mexico, ROTSE-I consisted of co-mounted telephoto lenses positioned in a four-fold array fixed on a rapid slewing mount. Each had a thermoelectrically cooled unfiltered 2048x2048 pixel Thompson TH7899 CCD. Filters were not used in order to improve measurement sensitivity. Apart from the CCD, each telescope contained a Canon FD 200 mm f/1.8 telephoto lens [6]. The four-fold array provided a 16°x16° wide field of view with each component telescope having a 64 square degree view. Depending on sky conditions, the ROTSE-I telescope would have a limiting magnitude of 14.5 - 15.5, which fell within the range of several other projects such as the Catalina Real-Time Transient Survey (CRTS) and the Wide Angle Search for Planets (SuperWASP) [9]. ROTSE-I was active from March 1998 to December 2001. During each night of observations, the telescope scanned the available sky, taking two 80 second exposures at predetermined sky patrol locations. This sequence occurred twice a night, covering approximately 18,000 degrees of the sky [5]. During its operational life cycle, ROTSE-I amassed a seven terabyte time domain survey. Of the 160 fields monitored, 9 were used in this study. However, for the VSP, the raw images were absent with only the ROTSE match structures being readily available. Data reduction consisted of four steps: instrument calibration, frame correction, astrometric calibration, and photometric calibration. For instrument calibration, a global dark frame and night sky flatfield were created each night automatically. Along with the 80 second exposures captured during sky patrol, 12 dark frames were taken every night with each set being median averaged to produce a global dark for the associated night. Flatfields were acquired by median averaging a single image of each patrol field. Once this calibration was done, the frames were used to correct the sky exposures. The global darks were subtracted from each image taken on their respective night with the flatfields subsequently applied [5]. Before astrometric and photometric calibration takes place, an object list was created from the now corrected images by using Source Extractor (SExtractor). The objects were then calibrated by matching sources from the images to those with matching right ascension (RA) and declination (DEC) from the Tycho astrometric catalogue [5].

2.2 ROTSE-III operation

The ROTSE-III telescope array is a network of robotic, automated telescopes, placed in Coonabarabran, Australia; Ft. Davis, Texas; Mt. Gamsberg, Namibia; and Bakirlitepe, Turkey, designed to search for Gamma-Ray bursts and other optical-band phenomena. Each one has a Cassegrain structure with a 0.45m f/1.8 primary mirror and a field corrector incident on a Marconi 2048x2048 back-illuminated thinned CCD. They have a 1.85°x1.85° field of view, which operates without a filter, with a passband that peaks around 550 nm [1]. Possible variables are constrained by a limiting magnitude of 17.5-19 depending on weather conditions and exposure times. A limiting magnitude of 17 can be reached with a 5s exposure, 18.5 with a 60s exposure and 19 by stacking images on top of each other, in a process called coadding. During patrolling nights ROTSE-III takes two pairs of 60s images at a 30-minute cadence. Observation requests are then stored in a prioritized queue with GRB alerts having the highest importance. Raw images, along with six darks at each exposure length, are stored and later used to create match structures during analysis [2]. The fields analyzed in this study were specifically scheduled for the VSP.

ROTSE-III data reduction follows a similar scheme to that of ROTSE-I. Calibration begins with the establishment of a median dark. The six darks taken each night are median averaged to form a master dark. Twilight flatfields are used for ROTSE-III instrument calibration as opposed to the night sky flats of its predecessor. Approximately 30 images of high elevation fields at twilight, away from sunset, are taken and median averaged. After the master frames are in hand, image correction is done. The master dark is subtracted from each image with the result being divided by the twilight flat field [10]. This process produces a corrected image which is compressed and saved in a ".fit" file. Data stored by ROTSE-III are carried in FITS files; denoting files stored in A Flexible Image Transport System (.fit). Before calibration continues, an object list is created for each corrected image with the SExtractor package. Information such as object number, aperture magnitude, and error are stored in a "sobj.fit" file. Data reduction proceeds with object calibration. Sources in the "sobj.fit" file are compared against those from the USNO A2.0 astrometric catalog [10]. The resulting corrected objects are saved to a new file, "cobj.fit" which is later used with their corresponding corrected images to produce a ROTSE match structure. Photometric calibration is achieved during the formation the match structure. All remaining analysis procedures are done off-line with IDL programs and C Shell commands. Two fields, VSP2218+4034 and SPV1724+3528, were used to develop the process for a widespread variable search in ROTSE-III. The coordinates in the names represent the center location of the field.

3. Data Analysis

All corrected image data from ROTSE-I and ROTSE-III are converted into ROTSE match structures before candidate identification. These structures contain data about every individual object, matched by position over a series of exposures, detected in the monitored fields. They also allow for easy data manipulation when making statistical variation cuts during light curve production. The ROTSE-I data used in this study had match structures previously created and did not require a reprocessing. Since ROTSE-III had not been previously searched for non-CV variables, the ROTSE match structures needed to be developed. As such, this analysis will focus on the ROTSE-III process. Each night of observations, for a given field, has its images checked to verify they are free from defects. We then constructed ROTSE match structures, using the previously obtained corrected images and object lists, with Relative Photometry (RPHOT), an IDL program. This program performs relative photometry on a specific optical transient (OT) as well as other nearby objects. It was designed with the ability for the user to easily oversee and make changes to a step in the data processing at any given moment [8]. A ROTSE match structure of the selected star and all reference stars is created from the inputted data. Each night of observations has its own unique structure.

3.1 Challenges and Solutions

It was discovered RPHOT was only able to process a maximum of approximately 1100 objects (including reference stars) at a time. The original intention of the program was for creating a light curve of a single OT. Instead, we were attempting to use it to process every object in the field. Depending on image size, each observation contained upwards of 9000+ objects. As a temporary solution, we created sub-images of the larger observation. To find the ideal sub-image size, multiple versions are each tested for the number of objects. Different sizes are checked until the threshold radius, is found. This is the radius that will contain around 1050 objects. Since each image may be cropped differently, object numbers tend to fluctuate. As a result, finding a size with 1100 objects is not optimal. Once the threshold is ascertained, the cuts are planned to ensure no parts of the image are omitted. If needed, the sub-image radius is lowered from the threshold to allow for the entire image to be used. Each field has a different

concentration of objects. Thus, a new sub-image size must be tested each iteration. All our ROTSE-III discoveries utilized this method.

3.2. Variable ID

After a ROTSE match structure for each night in a field is obtained, the process for identification of a potential variable in ROTSE-I and ROTSE-III becomes identical. A postscript file with light curves for each object identified in the field is created. Not all objects tracked have significant variation, thus, statistical cuts are made to the structure requiring phase plots meet certain criteria before they are printed. This process reduces the number of displayed curves that have to then be examined by eye. Both the filtering and generation of light curves from object data in the structures are done with an IDL program, "find_burst". By applying user set requirements on three central properties pertaining to light curves, "find_burst" searches and filters the ROTSE match structures accordingly. The used parameters are amplitude of magnitude variation (Δm), significance of maximum variation (σ_{max}), and chi-squared (χ^2) calculated over all measurements. Two of the three parameters account for error in magnitude measurements.

Magnitude variation (Δm) is calculated by subtracting the brightest observed magnitude from the dimmest for the light curve:

$$\Delta m = m_{max} - m_{min} \tag{1}$$

This variable is set as 0.1 in our analysis with *find_burst*. Light curves that do not meet Δm ≥ 0.1 are excluded from consideration.

The significance of maximum variation (σ_{max}) is calculated by dividing the difference in magnitude by the magnitudes' estimated uncertainties summed in quadrature:

$$\sigma_{max} = \Delta m/(\varepsilon_{max}{}^2 + \varepsilon_{min}{}^2)^{1/2} \tag{2}$$

Magnitude of the light curve is defined by *m* with ε being the estimated uncertainty for magnitude. This parameter is set as 1.0 in *find_burst*. The parameter compares the observed variation to the measurement errors checking to see if the former is much larger compared to the latter.

Chi-squared (χ^2) tests the agreement between the measurement distribution and the expected gaussian distribution for the measurements:

$$\chi^2 = \sum_{i=1}^{n} (m_i - \overline{m}_i)^2/\sigma_i \tag{3}$$

The summation is performed over all measurements. If the found χ^2 value is small, the light curve shows little to no variation. For variables, we expect χ^2 to be large. For our analysis, this parameter is set as 2.0.

Currently, the set values of the three variables are, respectively, 0.1, 1.0, and 2.0. Different parameter values were tested by Fagg et al. (2009) with our current set later becoming the standard [11]. Once "find_burst" is applied, a postscript file is outputted with light curves of objects that made the statistical cut. An example of the output is seen in **FIGURE 2**. This process is repeated for each night's match

structure. The result is a set of light curves for many objects over subsequent nights in which variational patterns can be recognized.

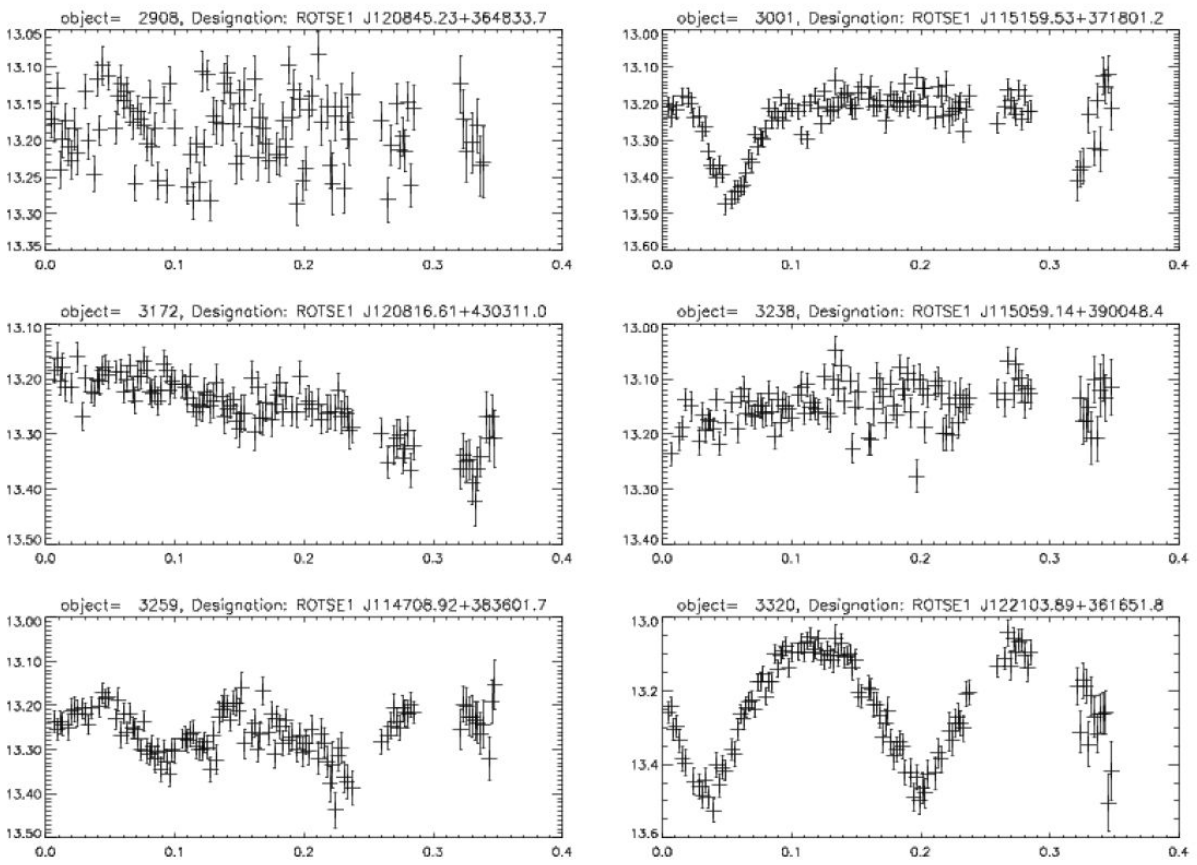

Figure: 2 Example light curves for a single night of observations.

Visual inspection for potential variable candidates begins by observing every light curve of a single night for any trends. Not all plots show obvious variation. If an object is seen as interesting, the coordinates and object number are noted and tracked over all following nights. After the follow-up, if the object continued to show signs of variation, the process for variable confirmation is initiated.

4. Variable Confirmation & Classification

As with initial identification, the confirmation stage is identical for both ROTSE data sets. Data on the object of interest is retrieved from the match structure of each night and concatenated into a single file to be phased together. This process combines each individual light curve to form a single one from multiple nights of data. The gathered data points are created depending on their grouping. ‘Good’ points were classified as those analyzed and given flags depending if the neighboring points were bright and close enough to bias the photometry, or if they were surrounded by bad pixels, with more than 10% of the integrated area affected [4]. After passing through two levels of cuts, one being more stringent than the other, the algorithm prints the data to the standard output if 20 or more points are cleared. With the data amassed, the best fitting period and amplitude of the folded light curve are found with a least-squares cubic spline fit algorithm developed in IDL [11]. The candidate’s light curve is produced, which displays

best fit period and amplitude in brightness variation values. The folded light curve is inspected to determine if the object shows enough variation to be classified. If the object is a suspected variable, further data points are gathered from public releases by other transient search projects such as SuperWASP and CRTS. Those data are combined with ROTSE data and the cubic spline fit is applied again. Other data sources help constrain the period and light curve shape. Once the elements have been improved and we possess the aggregated light curve, the variable is ready for type classification. The plots are reviewed for telling characteristics such as asymmetric peaks with steep ascending branches or a clean sinusoidal nature. Indication as to whether the variable is intrinsic or extrinsic along with a preliminary type comes from the initial inspection. Type is confirmed by checking if the period and amplitude of variations matches with the appropriate variable star prototype. If there are lingering doubts, in those cases, the spectral class of the variable components are determined and checked to ensure proper assignment.

Once a folded light curve with supporting datasets has been produced, steps can be taken to prepare the star for VSX submission. Supporting names from other telescopes such as 2MASS, WISE and USNO are added. Then the variability type, magnitude range, period, epoch, rise/eclipse duration are added in tandem with supporting papers and plots. The star is then passed to a registered moderator who reviews the data and variability type, and cites additional sources if need be. They document any changes that must be made to the submission, and communicate these to the original submitter. The history of changes and updates is logged so that VSX users can see when and why changes occurred to a particular variable. Once the dataset and submission is deemed satisfactory by the moderator, it is accepted as a variable star discovery and becomes searchable by the public. The submission is granted a unique identifier (AAVSO UID) which can be referenced to retrieve any version of the variable star's data. Existing entries can later be withdrawn or edited by moderators to include additional data sets or revisions as needed.

4.1 Variable Types

4.1.1 W UMa-Type (EW)

The most common variable star type found in the ROTSE All-Sky Survey, is W Ursae Majoris-types which are near contact binaries. Consisting of two components, each star's Roche lobes are overfilled resulting in both cores eventually being enclosed by a single common convective envelope. Classified by their light curves, W UMa-types are characterized by a sinusoidal nature with continuous variation. There is little to no difference between primary and secondary minima as result of the common envelope's equalized effective surface temperature [12]. Star components mainly belong to A-G spectral class. Variable periods are typically shorter than a day with the amplitude of variation being smaller than 0.8 magnitude [3].

4.1.2 RR Lyrae

RR Lyrae-type are intrinsic variables with a single component. The star's envelope contracts and expands in an attempt achieve hydrostatic equilibrium between pressure and gravity. Equilibrium is never achieved resulting in oscillation. This type is found where the instability strip, a diagonal region on the Hertzsprung-Russell diagram ranging from late A to K spectral class stars, crosses the horizontal branch. These variables commonly pulsate in their dominating fundamental mode. Light curves for RR Lyrae-type are visibly asymmetric, a result of the phase lag between radius and temperature change, with steep ascending branches and a slow descent in magnitude [13]. Subtypes found in our survey include both AB and C.

4.1.3 Delta Scuti

Delta Scuti variables (DSCT) are intrinsic variables that share the same pulsation mechanism as the RR Lyrae. Located on the instability strip where the region intersects with the main sequence, these variables exhibit radial as well as non-radial pulsation. In non-radial pulsation, there is no uniform expansion or contraction. Different parts of the star could be expanding while others are contracting. Thus, oscillation in overtone modes can occur simultaneously with or without the fundamental mode [14]. As a result, the light curves for this class of variables varies greatly depending on subtype and oscillation mode. A common subtype encountered in our candidate identification are High-amplitude Delta Scuti (HADS). These are DSCT radial pulsators with a light amplitudes >0.15 magnitudes in V [3].

5. Results

Across both R1 and R3 a total of 102 variables have been discovered. The VSP began with a focus on ROTSE-I variables, and of the total variables discovered, 82 have come from ROTSE-I. Two discoveries were updates to previous VSX entries that did not have complete supporting data. The objects tracked had a wide variety of supporting datasets from other telescopes due to ROTSE-I's lower limiting magnitude value:

Table 1:ROTSE-I Variable Star Discoveries

NAME	Constellation	Type	Magnitude Range	Period [d]
ROTSE1 J000044.33+375034.2	Andromeda	RRC	13.1 - 13.6 (R1)	0.291527
ROTSE1 J000231.95+340652.1	Andromeda	EW	14.3 - 15.0 (R1)	0.259568
ROTSE1 J000323.73+352856.9	Andromeda	EW	12.85 - 13.06 (R1)	0.394300
ROTSE1 J000349.50+315316.0	Pegasus	EW	12.63 - 12.78 (R1)	0.438080
ROTSE1 J000459.91+233315.0	Pegasus	ELL	11.97 - 12.07 (R1)	0.389094
ROTSE1 J000534.65+344449.0	Andromeda	EA	13.05 - 13.34 (R1)	0.466407
ROTSE1 J000546.47+331545.1	Andromeda	EW	13.15 - 13.38 (R1)	0.358822
ROTSE1 J000605.74+233938.4	Pegasus	EW	14.74 - 15.15 (R1)	0.291839
ROTSE1	Andromeda	EW	13.09 - 13.28 (R1)	0.413161

J000613.55+362658.0				
ROTSE1 J000755.84+333920.2	Andromeda	EW	12.42 - 12.61 (R1)	0.319604
ROTSE1 J000831.43+223154.8	Pegasus	EW	13.81 - 14.10 (R1)	0.399686
ROTSE1 J001118.58+232757.4	Andromeda	EA	12.53 - 12.78 (R1)	0.663242
ROTSE1 J001702.18+352707.6	Andromeda	ELL	11.71 - 11.79 (R1)	0.390897
ROTSE1 J002542.98+310715.1	Andromeda	EB	12.86 - 13.12 (R1)	0.613404
ROTSE1 J003005.66+344643.0	Andromeda	EA	14.0 - 14.6 (R1)	0.948832
ROTSE1 J110157.57+460657.9	Ursa Major	EA	13.30 - 13.70 (R1)	0.586194
ROTSE1 J110823.60+495250.5	Ursa Major	EW	11.85 - 11.99 (R1)	0.4318
ROTSE1 J111105.45+381123.5	Ursa Major	E	13.01 - 13.43 (R1)	n/a
ROTSE1 J111340.03+424413.8	Ursa Major	E	12.42 - 12.94 (R1)	n/a
ROTSE1 J111415.57+371825.6	Ursa Major	DSCT	12.92 - 13.12 (R1)	n/a
ROTSE1 J111719.74+394303.0	Ursa Major	EA	11.67 - 12.29 (R1)	n/a
ROTSE1 J112148.60+405938.4	Ursa Major	EW	13.16 - 13.33 (R1)	0.371699
ROTSE1 J112205.64+464333.5	Ursa Major	EB	11.68 - 12.05 (R1)	0.896686
ROTSE1 J112206.29+375441.9	Ursa Major	EW	13.46 - 13.61 (R1)	0.296779
ROTSE1 J112431.65+460702.7	Ursa Major	EW	14.30 - 14.90 (R1)	0.2947
ROTSE1	Ursa Major	EW	12.11 - 12.18 (R1)	0.416092

J112544.75+484255.8				
ROTSE1 J112944.11+355703.2	Ursa Major	ELL	12.01 - 12.09 (R1)	0.480146
ROTSE1 J113011.65+393043.2	Ursa Major	EW	12.48 - 12.58 (R1)	0.369101
ROTSE1 J113130.67+475420.8	Ursa Major	EW	13.00 - 13.30 (R1)	0.2480
ROTSE1 J114708.82+383602.3	Ursa Major	EW	13.21 - 13.32 (R1)	0.27908
ROTSE1 J115128.40+493130.5	Ursa Major	EW	11.63 - 11.72 (R1)	0.395714
ROTSE1 J115159.50+371801.3	Ursa Major	EA	13.16 - 13.45 (R1)	0.518288
ROTSE1 J115925.06+382405.1 (NSV 19084)	Ursa Major	RRAB	11.32 - 11.47 (V)	0.689474
ROTSE1 J115939.37+432236.3	Ursa Major	EW	14.25 - 14.70 (R1)	0.417234
ROTSE1 J120809.03+503321.7	Ursa Major	EW	12.07 - 12.17 (R1)	0.311734
ROTSE1 J122729.50+474420.0	Canes Venatici	EW/RS	12.83 - 13.03 (R1)	0.272838
ROTSE1 J154029.89+453200.6	Bootes	EW	12.86 - 13.16 (R1)	0.2643
ROTSE1 J161803.41+420417.4	Hercules	EB	11.32 - 11.52 (R1)	0.3230
ROTSE1 J162220.64+412400.7	Hercules	EW/RS	11.80 - 12.05 (R1)	0.4318
ROTSE1 J223159.77+135641.9	Pegasus	DSCT	13.00 - 13.16 (V)	0.115455
ROTSE1 J223452.37+175210.5	Pegasus	EW	12.13 - 12.28 (R1)	0.360692
ROTSE1 J230013.01+130716.7	Pegasus	EW	13.50 - 13.67 (R1)	0.239455

ROTSE1 J230032.53+080446.6	Pisces	EW	12.60 - 12.78 (V)	0.369126
ROTSE1 J230059.55+182723.9	Pegasus	EA	12.70 - 13.10 (V)	1.300850
ROTSE1 J230306.48+211614.1	Pegasus	EW	13.99 - 14.34 (R1)	0.447336
ROTSE1 J232208.37+135629.0	Pegasus	EW	12.63 - 12.81 (V)	0.421617
ROTSE1 J232605.82+233719.5	Pegasus	EB	12.94 - 13.17 (V)	0.700826
ROTSE1 J233046.35+130216.9	Pegasus	EW	12.35 - 12.48 (V)	0.288246
ROTSE1 J223707.20+212657.9	Pegasus	EW	12.08 - 12.17 (V)	0.281515
ROTSE1 J224742.62+114830.8	Pegasus	EA	10.65 - 10.97 (V)	3.115996
ROTSE1 J231114.24+083319.0	Pegasus	EW	14.04 - 14.33 (R1)	0.278611
ROTSE1 J231845.13+373527.2	Andromeda	EB	14.2 - 15.0 (R1)	0.457403
ROTSE1 J232049.49+250633.7	Pegasus	EW	13.25 - 13.38 (R1)	0.380810
ROTSE1 J232056.45+345150.9	Pegasus	HADS(B)	13.26 - 13.50 (R1)	0.109247
ROTSE1 J232109.31+170125.6	Pegasus	EW	12.50 - 12.63 (V)	0.251894
ROTSE1 J232708.22+371216.9	Andromeda	HADS	12.84 - 12.99 (R1)	0.084457
ROTSE1 J232953.24+263620.5	Pegasus	EW	12.78 - 13.07 (R1)	0.301900
ROTSE1 J234140.88+314655.7	Pegasus	EW	10.51 - 10.61 (R1)	0.367052
ROTSE1 J234514.63+275737.7	Pegasus	EA	12.58 - 13.80 (R1)	0.843388

ROTSE1 J235035.26+331853.7	Andromeda	EW	13.46 - 13.75 (R1)	0.267270

Of the ROTSE-I discoveries, 41 of the 82 are EW type variables, likely due to the short-period nature of these star systems, with periods shorter than one day being the most common. This accommodated ROTSE's shorter patrol period, as stars with longer variability periods would have to be purposefully tracked over several nights in order to accumulate enough data. The binary characteristics of EW systems allow for the mass, temperature and luminosity ratios of each star to be determined, as demonstrated by the following equations below.

For ROTSE-I objects, the quantum efficiency is maximum in the V-band, which allows us to calibrate the photometry as if a V-band filter were employed. Thus, the rotse magnitude and the Veff magnitudes can be considered to be roughly equivalent for the purposes of the following EW calculations. Using the phase plot submitted to VSX, the luminosity ratio of the EWs was able to be calculated:

$$\Delta m = m_{lim1} - m_{lim2} = \frac{L_{min1}}{L_{min2}} - 1$$

Where Δm is the difference, if any, in magnitude values between the two troughs of the EW. This allows us to calculate the mass ratio of the stars in the binary system via:

$$\frac{L_{min1}}{L_{min2}} = (\frac{M_1}{M_2})^{a} \qquad (1 < a < 6)$$

Where *a* is a parameter set to $a = 4$ as a value of four is valid for the range of stellar masses $(0.43M_{\odot} < M < 2M_{\odot})$ for the W UMa-type contact binaries **[D NEBOJSA SOURCE]**. With the luminosity ratio, the temperature ratio of the EW system could also be solved.

$$\frac{L_{min1}}{L_{min2}} = (\frac{T_1}{T_2})^4$$

Next, we calculate the absolute magnitude (*Mv*) for W UMa-type contact binaries using the following empirical relationship, described by Rucinski and Duerbeck [**Rucinski SOURCE**].

$$M_v = -4.44log(P) + 3.02(B-V)_0 + 0.12$$

Where *P* is the variable star's period. The effective temperature of the variable may be calculated using the B-V term from the previous equation:

$$T = 4600(\frac{1}{0.92(B-V)+1.7} + \frac{1}{0.92(B-V)+0.62})$$

Finally, a distance estimate to the star may be calculated in units of parsecs:

$$m - M = 5[log_{10}(d) - 1]$$

Where *m* is the apparent magnitude, and *M* is the absolute magnitude, which for any object outside the solar system is the apparent magnitude it would have if it were located at a distance of 10.0 parsecs. The uncertainty in the distance calculations is systematic, which consists of several contributing factors:

1. 0.1 magnitude: phase at half amplitude
2. 0.2 magnitude: USNO photometry
3. 0.2 magnitude: m_{rotse} correlation of $V \Rightarrow V_{eff}$ (half of width)

The sum in quadrature of these uncertainties is calculated by the following steps:

$$\delta d = \sqrt{(0.1)^2 + (0.2)^2 + (0.2)^2} = 0.30 \Rightarrow d \pm \delta d = d \pm 30\%$$

Using these parameters we can characterize the EW variables discovered through the ROTSE-I survey.

Table 2: EW Parameters

Star	Period [d]	B (band)	Veff	B-Veff	Mv	Delta m	L1/L2	T1/T2	Teff [Kelvin]	m1/m2	distance [parsecs]	distance error
ROTSE1 J000231.95+340652.1	0.259568	15.409	14.3	1.109	6.0699	0.1	1.1	1.02411	4495.40165	1.1	442.60875	132.78263
ROTSE1 J000323.73+352856.9	0.394300	13.760	12.85	0.91	4.66273	0.025	1.025	1.00619	4969.76118	1.025	433.9643	130.18929
ROTSE1 J000349.50+315316.0	0.438080	13.165	12.63	0.535	3.3272	0.05	1.05	1.01227	6234.29546	1.05	725.37068	217.6112
ROTSE1 J000546.47+331545.1	0.358822	13.575	13.15	0.425	3.37984	0	1	1	6749.8549	1	899.56386	269.86916
ROTSE1 J000604.33+345612.8	0.395747	14.690	14.30	0.39	3.08527	0.05	1.05	1.01227	6933.94345	1.05	1749.62913	524.88874
ROTSE1 J000605.74+331545.1	0.291839	15.503	14.74	0.763	4.79902	0.08	1.08	1.01943	5394.78435	1.08	973.18633	291.9559
ROTSE1 J000613.55+362658.0	0.413161	13.470	13.09	0.38	2.97203	0	1	1	6988.56478	1	1055.83001	316.749
ROTSE1 J000755.84+333920.2	0.319604	12.966	12.42	0.546	3.96844	0	1	1	6187.35925	1	490.13081	147.03924
ROTSE1 J000831.43+223154.8	0.399686	14.023	13.81	0.213	2.53163	0	1	1	8063.74277	1	1801.66483	540.49945
ROTSE1 J001058.53+354034.0	0.304429	15.494	14.34	1.154	5.8984	0.05	1.05	1.01227	4401.01267	1.05	487.88785	146.36636
ROTSE1 J110823.60+495250.5	0.4318	12.353	11.85	0.503	3.25841	0.025	1.025	1.00619	6375.31414	1.025	522.77884	156.83365
ROTSE1 J112148.80+405938.4	0.371699	13.704	13.16	0.544	3.67123	0.025	1.025	1.00619	6195.8364	1.025	790.23089	237.06927
ROTSE1 J112206.29+375441.9	0.296779	14.420	13.46	0.96	5.3616	0.05	1.05	1.01227	4840.87544	1.05	416.56234	124.9687
ROTSE1 J112431.65+460702.7	0.2947	15.249	14.3	0.949	5.34193	0.125	1.125	1.02988	4868.62055	1.125	618.89076	185.66723
ROTSE1 J112544.75+484255.8	0.416092	13.971	12.11	1.861	7.43102	0	1	1	3320.58972	1	86.25733	25.8772
ROTSE1 J113011.65+393043.2	0.369101	12.756	12.48	0.276	2.8754	0	1	1	7617.88142	1	833.52763	250.05829
ROTSE1 J113130.67+475420.8	0.2480	13.959	13.0	0.959	5.70481	0.1	1.1	1.02411	4843.38391	1.1	287.76502	86.32951
ROTSE1 J114708.82+383602.3	0.27908	13.678	13.21	0.468	3.99432	0.05	1.05	1.01227	6537.67389	1.05	696.8447	209.05341
ROTSE1 J115128.40+493130.5	0.395714	12.105	11.63	0.475	3.34213	0.025	1.025	1.00619	6504.48976	1.025	454.54198	136.36259
ROTSE1 J115939.37+432236.3	0.417234	14.748	14.25	0.498	3.30947	0	1	1	6397.97346	1	1542.07679	462.62304
ROTSE1 J120809.03+503321.7	0.311734	12.537	12.07	0.467	3.77794	0	1	1	6542.44442	1	455.4199	136.62597
ROTSE1 J122729.50+474420.0 [EW/RS]	0.272838	13.722	12.83	0.892	5.31842	0.025	1.025	1.00619	5017.95867	1.025	317.91865	95.3756
ROTSE1 J154029.89+453200.6	0.2843	13.986	12.86	1.126	5.94575	0.04	1.04	1.00985	4459.24769	1.04	241.46267	72.4388

ROTSE1 J162220.64+412400.7 [EW/RS]	0.4139	12.783	11.79	0.993	4.81984	0	1	1	4759.60801	1	247.76046	74.32814
ROTSE1 J223452.37+175210.5	0.360692	12.860	12.13	0.73	4.29091	0	1	1	5501.09296	1	369.67323	110.90197
ROTSE1 J223707.20+212657.9	0.281515	12.994	12.08	0.914	5.32449	0	1	1	4959.18343	1	224.4409	67.33227
ROTSE1 J230013.01+130716.7	0.239455	14.553	13.50	1.053	6.05631	0.05	1.05	1.01227	4618.9867	1.05	308.13285	92.43986
ROTSE1 J230032.53+080446.6	0.369126	13.366	12.60	0.766	4.35506	0	1	1	5385.33653	1	445.64393	133.69318
ROTSE1 J230306.48+211614.1	0.447336	15.391	13.99	1.401	5.90221	0.05	1.05	1.01227	3948.75698	1.05	414.53194	124.35958
ROTSE1 J231704.72+371849.0	0.331355	11.517	10.98	0.537	3.87164	0.025	1.025	1.00619	6225.70459	1.025	264.04138	79.21241
ROTSE1 J232112.70+134735.2	0.289972	14.816	13.62	1.196	6.11906	0.1	1.1	1.02411	4316.59054	1.1	316.36469	94.90941
ROTSE1 J232208.37+135629.0	0.421617	13.103	12.63	0.473	3.21382	0.05	1.05	1.01227	6513.9337	1.05	764.25097	229.27529
ROTSE1 J232049.49+250633.7	0.380810	13.691	13.25	0.441	3.31347	0.05	1.05	1.01227	6669.18064	1.05	971.19402	291.35821
ROTSE1 J232953.24+263620.5	0.301900	13.535	12.78	0.755	4.70951	0.1	1.1	1.02411	5420.15214	1.1	411.24251	123.37275
ROTSE1 J233046.35+130216.9	0.288246	13.244	12.35	0.894	5.21853	0	1	1	5012.55453	1	266.86646	80.05994
ROTSE1 J231114.24+083319.0	0.278611	14.532	14.04	0.492	4.07005	0.05	1.05	1.01227	6425.39544	1.05	986.25678	295.87703
ROTSE1 J232109.31+170125.6	0.251894	13.362	12.50	0.862	5.38183	0.05	1.05	1.01227	5100.52949	1.05	265.23693	79.57108
ROTSE1 J233257.40+333850.5	0.290538	10.717	10.15	0.567	4.21572	0	1	1	6099.83368	1	153.76447	46.12934
ROTSE1 J234140.88+314655.7	0.367052	N/A	10.51			0.01	1.01	1.00249		1.01		
ROTSE1 J235035.26+331853.7	0.267270	N/A	13.46			0	1	1		1		
ROTSE1 J235855.86+334133.7	0.341347	14.494	13.82	0.674	4.22809	0	1	1	5692.12835	1	828.67073	248.60122
ROTSE3 J172014.15+352919.1	0.455322	13.111	12.21	0.901	4.35809	0.075	1.075	1.01824	4993.73675	1.075	371.86217	111.55865
ROTSE3 J180829.49-203047.8	0.3813	16.286	14.8	1.486	6.4669	0	1	1	3814.6863	1	464.10901	139.2327
ROTSE3 J221525.73+403113.1	0.312335	17.417	16.0	1.417	6.64322	0.2	1.2	1.04664	3922.77497	1.2	743.62846	223.08854
ROTSE3 J221536.49+411129.5	0.399237	13.683	12.63	1.053	5.0706	0	1	1	4618.9867	1	324.99748	97.49924
ROTSE3 J221545.32+395017.9	0.328687	14.135	13.03	1.105	5.60259	0.1	1.1	1.02411	4503.99821	1.1	305.83135	91.74941
ROTSE3 J221551.61+412030.1	0.286444	N/A	16.6			0	1	1		1		
ROTSE3 J221557.53+405956.3	0.264000	16.749	15.56	1.189	6.27886	0	1	1	4330.42436	1	718.17122	215.45137

ROTSE3 J221604.18+404715.5	0.477485	11.485	10.63	0.855	4.12752	0.025	1.025	1.00619	5120.21272	1.025	199.75424	59.92627
ROTSE3 J221822.13+400218.0	0.408050	14.963	14.15	0.813	4.30369	0	1	1	5241.78709	1	931.66976	279.50093
ROTSE3 J221904.59+395132.3	0.302588	17.115	16.35	0.765	4.73532	0	1	1	5388.48188	1	2103.46844	631.04053
ROTSE3 J222009.69+412042.3	0.374486	16.566	15.54	1.026	5.11247	0.05	1.05	1.01227	4681.16776	1.05	1217.60381	365.28114
ROTSE3 J222027.50+395316.8	0.331788	15.855	15.92	-0.065	2.05108	0.1	1.1	1.02411	11015.88912	1.1	5939.96656	1781.98997
ROTSE3 J222125.07+403412.9	0.36902	15.466	14.61	0.856	4.62742	0.05	1.05	1.01227	5117.39096	1.05	992.00989	297.60297
ROTSE3 J222137.37+405235.4	0.793211	14.990	14.38	0.61	2.40891	0.1	1.1	1.02411	5928.6628	1.1	2478.66595	743.59979
ROTSE3 J222210.88+404033.4	0.371922	16.076	15.31	0.766	4.34051	0	1	1	5385.33653	1	1562.78056	468.83417
ROTSE3 J222253.75+402458.7	0.373970	16.213	15.35	0.863	4.62286	0	1	1	5097.7307	1	1397.74517	419.32355

The image files from ROTSE-III contain a large amount of data within the fields; the recent discoveries from these telescopes were the first foray into the data set and thus only skim the surface in terms of possible discoveries. The greater limiting magnitude provided an ideal environment to submit variable star discoveries, as the dimmer the stars became, the less amount of supporting data from other telescopes proved to be available thus making first discoveries more feasible. The following stars were accepted as discoveries into VSX:

Table 3: ROTSE-III Variable Star Discoveries

Name	**Constellation**	**Type**	**Magnitude Range**	**Period [d]**
ROTSE3 J172014.15+352919.1	Hercules	EW	12.21 - 12.40 (R1)	0.455322
ROTSE3 J180829.49 -203047.8	Sagittarius	EW	14.80 - 15.50 (R1)	0.3813
ROTSE3 J221525.73+403113.1	Lacerta	EW	16.0 - 16.4 (R1)	0.312325
ROTSE3 J221532.62+402235.1	Lacerta	RRAB	14.40 - 15.20 (R1)	0.489555
ROTSE3 J221536.49+411129.5	Lacerta	EW	12.63 - 12.86 (R1)	0.399237
ROTSE3 J221545.32+395017.9	Lacerta	EW	13.03 - 13.60 (R1)	0.328687

ROTSE3 J221557.53+405956.3	Lacerta	EW	15.56 - 15.91 (R1)	0.264000
ROTSE3 J221604.18+404715.5	Lacerta	EW	10.63 - 10.79 (R1)	0.477485
ROTSE3 J221822.13+400218.0	Lacerta	EW	14.15 - 14.37 (R1)	0.408050
ROTSE3 J221904.59+395132.3	Lacerta	EW	16.35 - 16.70 (R1)	0.302588
ROTSE3 J222027.50+395316.8	Lacerta	EW	15.92 - 16.23 (R1)	0.331788
ROTSE3 J222115.63+403454.8	Lacerta	EB	16.25 - 16.94 (R1)	0.482016
ROTSE3 J222125.07+403412.9	Lacerta	EW	14.61 - 14.80 (R1)	0.369020
ROTSE3 J222137.37+405235.4	Lacerta	EW	14.38 - 14.83 (R1)	0.793211
ROTSE3 J222210.88+404033.4	Lacerta	EW	15.31 - 15.67 (R1)	0.371922
ROTSE3 J222253.75+402458.7	Lacerta	EW	15.35 - 15.56 (R1)	0.373970

As with ROTSE-I, the majority of the discoveries made were of EW type, and in the Lacerta constellation. 3 pulsator types were discovered, with two RRCs and one RRAB. ROTSE-III excels at discovering short period variables, thus all discoveries have periods listed under one day. Discovering long period variables would require specific tracking and is not currently necessary, as the image fields contain enough data to continue processing discoveries using the nightly sky patrols.

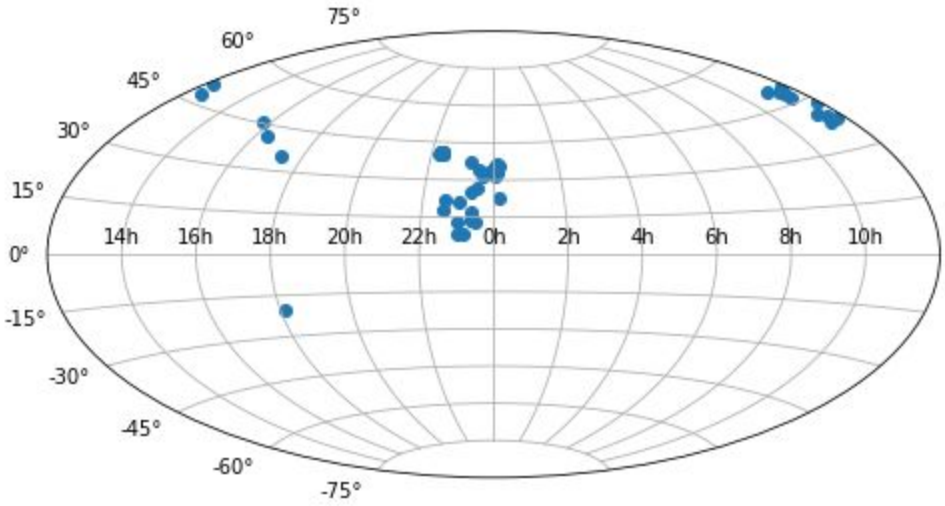

Fig XXX. Aitoff projection of R1 and R3 EW discoveries on the celestial sphere

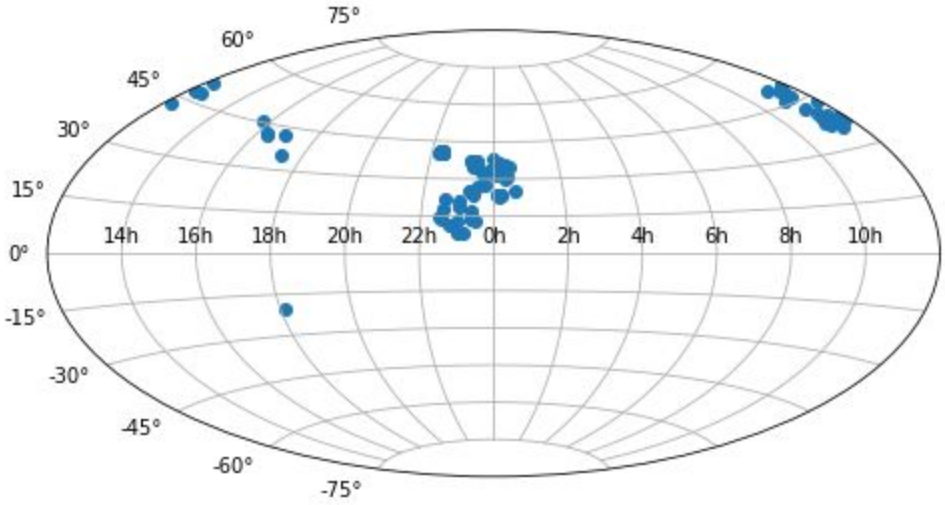

Fig XXX. Aitoff projection of all R1 and R3 discoveries on the celestial sphere

5.1 VSX Updates

In addition to processing data for the purpose of new variable star discoveries, the VSP project included updating entries in the VSX database that contained a relative lack of supporting data. One such example would be NSV 19084, which was a variable discovered several decades ago through A.Slettebak, J.Stock, Bergd Abh Bd.5, Nr.5, 1959. Despite its status as an accepted discovery, the database entry was missing the star's type, period, epoch, rise duration and maximum magnitude. Through use of ROTSE-I and supporting data sets, these missing factors were resolved and submitted alongside the star's phase plot. Thus, any further ROTSE data discoveries which yield supporting data to VSX entries that are not complete will also undergo the submission process to provide supporting information for already discovered variables.

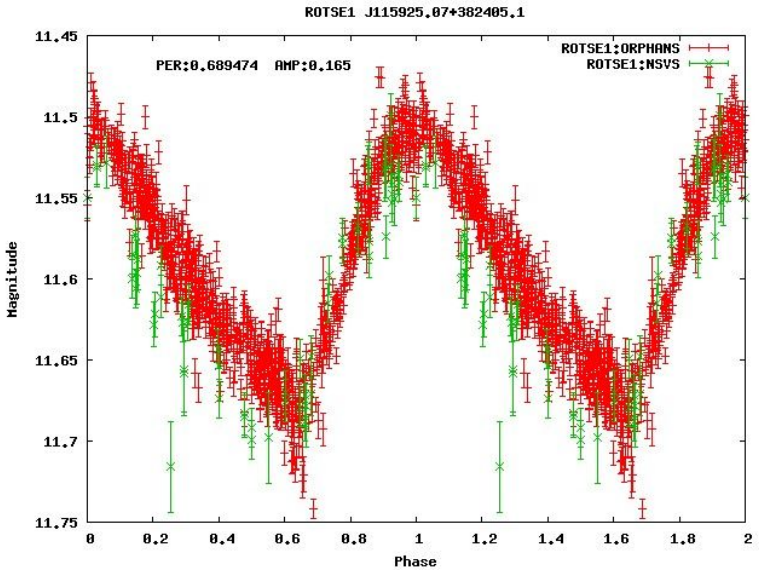

Figure XXX: Light Curve of NSV 19084 (ROTSE1 J115925.07+382405.1)

This also holds true for VSX entry V0487 And. Originally discovered in 2008 by M.L. Kuzmin from the NSVS public data release, ROTSE results were added in order to complete variable type, range, epoch, and period as collected from ROTSE-I Orphans, NSVS, and SuperWASP data. UCAC4 position was updated as well.

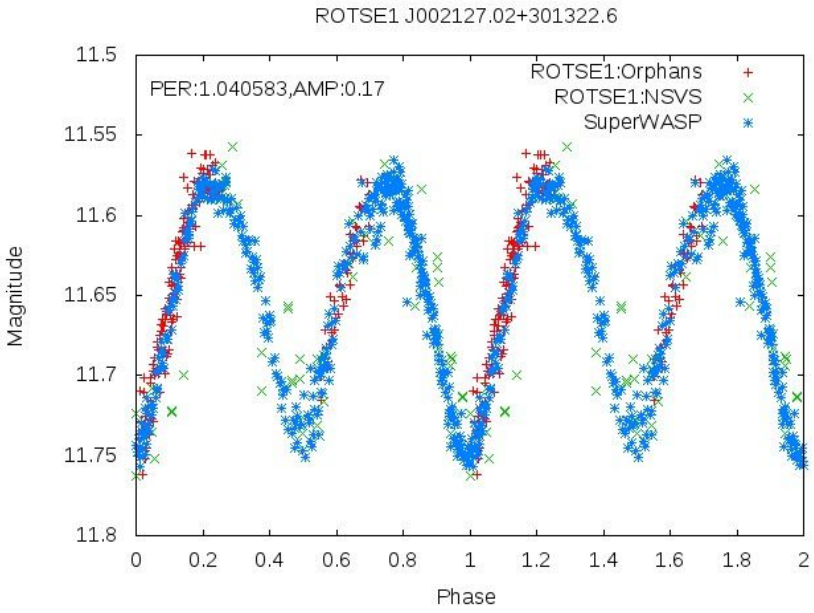

Figure XXX: Light Curve of V0487 And (ROTSE1 J002127.02+301322.6)

5.2 Blended Stars

In the discoveries made there are a few instances of finding a star with a close companion. Starlight from the companion contaminates the amplitude of variations of the variable candidate. This causes some issues and

6. Conclusion & Future Prospects:

The goal of the Variable Star Project was to identify and submit possible discoveries for VSX cataloging. We extended previously established techniques used for candidate selection in ROTSE-I data to the backlog of ROTSE-III data accumulated in the search for GRBs. New protocols were also enacted with ROTSE-III analysis to account for differences in available data and extra processes required to form match structures for each monitored field.

While new variables have been discovered in the ROTSE-III fields, the process for discovery is far from ideal and requires improvement. It is desired to make ROTSE-III fields as simple to analyze as its ROTSE-I counterpart. This will allow for the extended ROTSE team to make more contributions using terabytes of yet untouched data readily available.

References

[1] http://www.konkoly.hu/cgi-bin/IBVS?5559 (Bulletin containing R3 Info)

[2] http://iopscience.iop.org/article/10.1086/345490/pdf **(About ROTSE3 Telescope)**

[3] https://www.aavso.org/vsx/help/VariableStarTypeDesignationsInVSX.pdf

[4]https://drive.google.com/file/d/0B-eyNQAn-J4xRGdvdkhJMmFlbTg/view?usp=sharing **(Gettel Thesis.)**

[5]http://iopscience.iop.org/article/10.1086/301321/pdf (Fields paper)

[6]http://arxiv.org/pdf/astro-ph/9909219v1.pdf (Kehoe Prompt Optical...Has info on R1)

[7] Spline fit paper TBCited

[8] Quimby PhD Thesis. Has info on RPHOT:
https://www.lib.utexas.edu/etd/d/2006/quimbyr60956/quimbyr60956.pdf

[9] Farley's Thesis (VSX/Phasing)

[10] ROTSE 3 Manual http://www.rotse.net/equipment/docs/rotsedocs.pdf

[11] http://www.jurp.org/2009/ms108_111609.pdf Undergrad paper with info on statistical cuts

[12] W UMa-type Lucy's Paper. Structure of binary stars.

[13] RR Lyrae AAVSO Page info https://www.aavso.org/vsots_rrlyr

[14] D Scuti AAVSO Page info https://www.aavso.org/vsots_delsct

[15] D. Nebojsa, Advanced Astrophysics, Cambridge, MA: Cambridge University Press, 2004, p. 20.

[16] S. M. Rucinski and H. W. Duerbeck, "Absolute Magnitude Calibration for the W UMa-Type Systems Based on HIPPARCOS Data," *Publications of the Astronomical Society of the Pacific,* vol. 109, pp. 1340-1350, 1997.

[17] M. Zeilik and E. v. P. Smith, Introductory Astronomy & Astrophysics, New York, NY: Saunders College Publishing, 1987 (**Distance calc source**)

[18]http://articles.adsabs.harvard.edu/cgi-bin/nph-iarticle_query?1967MmRAS..70..111E&data_type=PDF_HIGH&whole_paper=YES&type=PRINTER&filetype=.pdf **(EW color-period relation [I think it was the first type of star to have this??])**

[Akerlof] C. Akerlof, C. Alcock, R. Allsman, T. Axelrod, D. P. Bennett, K. H. Cook, K. Freeman, K. Griest, S. Marshall, H. S. Park, S. Perlmutter, B. Peterson, P. Quinn, J. Riemann, A. Rodgers, C. W. Stubbs and W. Sutherland, "Application of cubic splines to the spectral analysis of unequally spaced data," ApJ, vol. 436, no. 2, pp. 787-794, December 1994